Antiapoptotic Activity Is Dispensable for Insulin-like Growth Factor I Receptor-mediated Clonogenic Radioresistance after γ-Irradiation[1]

Mikio Tezuka, Hiroshi Watanabe, Shin Nakamura, Dong Yu, Winn Aung, Takehito Sasaki, Hitoshi Shibuya, and Masahiko Miura[2]

Molecular Diagnosis and Therapeutics [M. T., D. Y., W. A., M. M.] and Oral and Maxillofacial Radiology [H. W., S. N., T. S.], Department of Oral Restitution, and Diagnostic Radiology and Oncology, Department of Head and Neck Reconstruction [M. T., D. Y., W. A., H. S.], Graduate School, Tokyo Medical and Dental University, Tokyo 113-8549, Japan

ABSTRACT

Purpose: **The purpose of this study was to evaluate the relationship between apoptotic activity and clonogenic radiosensitivity *in vitro* using an insulin-like growth factor I receptor (IGF-IR) signaling model, which is known to exert tumorigenic and antiapoptotic effects.**

Experimental Design: **We used mouse embryo fibroblast cell lines expressing either human IGF-IR [R+(Wt) and R+] or the marker gene alone [R−(puro)]; these cell lines were derived from R− cells, which are deficient in IGF-IR. After γ-irradiation, apoptotic activity was determined by the presence of DNA fragmentation and caspase-3-, -8-, and -9-like activities. Clonogenic radiosensitivity was determined by a colony-forming assay.**

Results: **R+(Wt) and R+ cells expressed similar levels of IGF-IR, transducing phosphorylation signals to major downstream substrates on insulin-like growth factor I stimulation. R+ cells were resistant to the induction of apoptosis after γ-irradiation; however, both R+(Wt) and R−(puro) cells demonstrated significant DNA fragmentation and increase in caspase-3-, -8-, and -9-like activities. Both R+(Wt) and R+ cells were radioresistant (to a similar extent) compared with R−(puro) cells as measured by a colony-forming assay. Clonogenic radioresistance was not influenced by the inhibition of Akt/protein kinase B through treatment with wortmannin at low concentrations specifically inhibiting phosphatidylinositol 3′-kinase.**

Conclusions: **Our findings indicate that apoptotic activity does not necessarily predict clonogenic survival after exposure to ionizing radiation. This study provides clinical implications in the evaluation of apoptotic activities observed during the course of radiotherapy to predict accurate tumor response or local control.**

INTRODUCTION

Apoptosis is an active cell suicide process exemplified by characteristic morphological changes and biochemical features distinct from necrosis (1–7). Although apoptosis is a fundamental biological aspect (8) of normal embryonic development (9) and aging (10), many additional stresses trigger this process (11–13). Because IR[3] (14, 15) and chemotherapeutic agents (16) frequently used for cancer treatment induce apoptosis of tumor cells, the prospect of enhancing patient responses by regulating apoptosis may improve current cancer therapies (17). However, the mechanism controlling the induction of apoptosis is likely to be both tissue and stimulus specific (18). This assumption suggests that the findings obtained using a given trigger in apoptosis-sensitive cells, such as hematopoietic cell lines, are not directly applicable to radiotherapy of solid tumors (19). Cells of solid tumors usually exhibit low apoptotic activity *in vitro* and *in vivo* after IR (at most, 20–30%; Refs. 20 and 21); the major mode of cell death is mitotic death, presumably necrosis (20). In cervical cancer, clinical studies have reported the relationship between prognosis and the incidence of apoptosis (AI) before or after radiotherapy. Spontaneous apoptosis before radiotherapy is not a significant prognosticator (22, 23), whereas Levine *et al.* (24) have reported that patients with a low spontaneous AI exhibited significantly higher survival rates. Patients with a high AI during the early stages of radiotherapy had a better prognosis; this increased survival was accompanied by a higher expression of proapoptotic factors, such as Bax (25). Thus, the relationship between AI and clinical response to radiotherapy for solid tumors is still unclear; therefore, studies using cell lines with low apoptotic activity are essential to clarify these issues.

The IGF-IR plays a pivotal role in cell growth, protection

Received 3/15/01; revised 6/28/01; accepted 7/5/01.
The costs of publication of this article were defrayed in part by the payment of page charges. This article must therefore be hereby marked *advertisement* in accordance with 18 U.S.C. Section 1734 solely to indicate this fact.
[1] Supported in part by Grants-in-Aid for Scientific Research (B) (10470399) and for Encouragement of Young Scientists (12771120) from the Japan Society for the Promotion of Science.
[2] To whom requests for reprints should be addressed, at Molecular Diagnosis and Therapeutics, Department of Oral Restitution, Graduate School, Tokyo Medical and Dental University, 1-5-45 Yushima, Bunkyo-ku, Tokyo 113-8549, Japan. Phone: 81-3-5803-5545; Fax: 81-3-5803-0205; E-mail: masa.mdth@tmd.ac.jp.

[3] The abbreviations used are: IR, ionizing radiation; IGF-I, insulin-like growth factor I; IGF-IR, IGF-I receptor; PKB, protein kinase B; PI3K, phosphatidylinositol 3′-kinase; IRS-1, insulin receptor substrate 1; MAPK, mitogen-activated protein kinase; AI, apoptotic index; HRP, horseradish peroxidase; ECL, enhanced chemiluminescence; AFC, 7-amino-4-trifluoromethyl coumarin; EGFR, epidermal growth factor receptor; ERK, extracellular signal-regulated kinase; DNA-PK, DNA-dependent protein kinase; ATM, ataxia telangiectasia mutated.

against apoptosis, and establishment and maintenance of a transformed phenotype (26–29); IGF-IR is overexpressed in some tumor cells, including breast cancer and glioblastoma cells (30, 31). After IGF-IR stimulation, the PI3K-associated survival signals lead to Akt/PKB and Bad transduction, protecting cells against apoptosis after a variety of stimuli (32, 33). Little is known, however, about IR-induced apoptosis. Mouse embryo fibroblasts with a targeted disruption of the *IGF-IR* gene (R−) undergo apoptosis (~20%) after IR; however, the major mode of cell death was necrosis (34). Apoptosis was significantly inhibited in cells overexpressing the IGF-IR (R+ cells) derived from R− cells, which are widely used as a positive control in IGF-IR-associated experiments (27, 35–38). This study did not examine clonogenic cell survival, a representative marker of radiosensitivity thought to reflect reproductive integrity of immortalized or tumor cells (19, 39). These results prompted the examination of the association of increased induction of apoptosis with clonogenic survival after IR. Elucidation of this relationship may have clinical implications for the radiotherapy of solid tumors.

Here we provide evidence that apoptotic activity and clonogenic radiosensitivity do not necessarily correlate *in vitro* using an IGF-IR signaling model. These data suggest that information obtained regarding the induction of apoptosis during a radiotherapeutic course should be interpreted carefully to predict tumor response.

MATERIALS AND METHODS

Cell Lines and Culture Conditions. R− cells, which were obtained from a mouse embryo possessing a null mutation of the *IGF-IR* gene (27), were cotransfected with a pBPV IGF-IR plasmid carrying the full-length coding region of human IGF-IR cDNA (27) and a pPDV6+ plasmid carrying the puromycin resistance gene (40) by calcium phosphate precipitation. Cells were selected in 4 μg/ml puromycin; the resulting clones were mixed. We analyzed the expression levels of IGF-IR in the mixed transfectants by flow cytometry; cells expressing high levels of IGF-IR were sorted under sterile conditions as described previously (35). The obtained mixed populations were designated R+(Wt) cells. Mixed populations transfected with the marker gene alone were designated R−(puro) cells. R+ cells, which were also derived from R−cells that were cotransfected with both the same human IGF-IR expression plasmid described above and a pLHL4 plasmid carrying the hygromycin resistance gene, were isolated after hygromycin selection (27). All cells were maintained at 37°C in a humidified atmosphere containing 5% CO_2 in Eagle's MEM containing 1 mM sodium pyruvate, 100 units/ml penicillin, and 100 μg/ml streptomycin supplemented with 10% fetal bovine serum.

IGF-IR Expression Levels. Cells were lysed in a lysis buffer [20 mM Tris-HCl (pH 7.5), 150 mM NaCl, 0.5% Triton X-100, 0.1% SDS, 1 mM EDTA, 100 mM NaF, 1 mM sodium orthovanadate, 1 mM phenylmethylsulfonyl fluoride, and 1 μg/ml aprotinin]. Equal amounts of whole cell lysates were resolved by SDS-PAGE. Proteins were transferred to a nitrocellulose membrane in a Tris-glycine buffer containing 20% methanol. After blocking with 5% nonfat milk in TBST [10 mM Tris-HCl (pH 7.5), 150 mM NaCl, and 0.1% Tween 20], filters were probed with antibodies against the α- and β-subunits of the IGF-IR (Santa Cruz Biotechnology, Santa Cruz, CA). After washing with TBST, filters were incubated with a HRP-conjugated antirabbit IgG (Santa Cruz Biotechnology) and visualized using the ECL system (Amersham, Arlington Heights, IL). As a loading control, filters were also probed with an anti-protein kinase C-δ antibody (Transduction Laboratories, Lexington, KY) and visualized using a secondary antibody (antimouse IgG conjugated with HRP; Santa Cruz Biotechnology) and the ECL system.

IGF-IR, IRS-1, and Shc Activation. To detect IGF-I-induced tyrosine phosphorylation of the IGF-IR and IRS-1, cells incubated in serum-free medium for 24 h in 100-mm plates were either left untreated or treated with 50 ng/ml IGF-I (Life Technologies, Inc., Gaithersburg, MD) for 10 or 15 min. Cells were lysed in the lysis buffer described above. Equal amounts of whole cell lysates were subjected to SDS-PAGE; the proteins were then transferred to a nitrocellulose filter as described above. After blocking with 5% nonfat milk solution, the filters were incubated with a HRP-conjugated anti-phosphotyrosine antibody (Upstate Biotechnology, Lake Placid, NY). Phosphotyrosines were visualized with the ECL system (Amersham). To detect IGF-I-induced tyrosine phosphorylation of Shc, untreated serum-starved cells or serum-starved cells treated with IGF-I as described above were lysed in a lysis buffer [20 mM Tris-HCl (pH 7.5), 150 mM NaCl, 1 mM EGTA, 1% Triton X-100, 2.5 mM Na PP_i, 1 mM β-glycerolphosphate, 1 mM sodium orthovanadate, 1 mM phenylmethylsulfonyl fluoride, and 1 μg leupeptin]. Equal amounts of protein were incubated for 1 h with an anti-Shc antibody (Transduction Laboratories) at 4°C and then incubated with protein A/G-agarose (Santa Cruz Biotechnology) for an additional hour. After three washes in lysis buffer, the immunoprecipitants were resolved using SDS-PAGE and transferred to nitrocellulose filters. Phosphorylated tyrosines of Shc were visualized as described for the detection of IGF-IR and IRS-1 phosphorylation.

MAPK and Akt/PKB Activation. Serum-starved cells either left untreated or treated with 50 ng/ml IGF-I were lysed in a lysis buffer [62.5 mM Tris-HCl (pH 6.8), 2% SDS, 10% glycerol, 50 mM DTT, and 0.1% bromphenol blue]. Activated proteins were visualized as described above using anti-ACTIVE MAPK (Promega, Madison, WI) and anti-PKB/Akt [pSer(473); Biosource, Camarillo, CA] as primary antibodies to detect the phosphorylated forms of MAPK and Akt/PKB, respectively. To examine the time course of MAPK and Akt/PKB activation after γ-irradiation, cells were γ-irradiated in growth medium at room temperature as described below. Irradiated cells were immediately transferred to an incubator at 37°C. Cells were lysed at the indicated times as described above and processed for Western blotting. Cells were also irradiated at 37°C; results were identical to those obtained at room temperature.

Cell Growth Assay. Cells (1×10^5) were plated in 60-mm dishes, and the number of cells was counted at the indicated times using a hemocytometer.

Tumor Growth in Nude Mice. Male KSN nude mice were purchased from Japan SLC Inc. (Hamamatsu, Japan), and experiments were carried out in accordance with the Guidelines for Animal Experimentation of Tokyo Medical and Dental University. To evaluate the tumorigenicity of each cell line, we

inoculated KSN nude mice s.c. in the right thigh with 100 μl of growth medium containing 5×10^5 cells. Tumor growth was monitored by palpation. The size of palpable tumors was measured with calipers every 3–4 days. The tumor volume (V; in mm^3) was estimated as V = length (mm) × [width^2 (mm)]/2.

Internucleosomal DNA Fragmentation. DNA fragmentation of γ-irradiated cells was visualized as described previously (34). Cells grown in eight 100-mm dishes containing 2×10^5 cells each were irradiated at a dose of 10 Gy. The floating dead cells were collected 72 h after irradiation by mixing the overlaying medium with media from washes of the remaining adherent cell layer. After a wash in PBS, the collected cells were resuspended with 20 μl of lysis buffer [50 mM Tris-HCl (pH 8.0), 10 mM EDTA, 0.5% sodium lauryl sarkosinate, and 0.5 mg/ml proteinase K]. After incubation at 50°C for 1 h, we added 10 μl of 0.5 mg/ml RNase A and incubated the mixture at 50°C for an additional hour. Ten μl of sample buffer [50 mM Tris-HCl (pH 8.0), 10 mM EDTA, 1% low melting temperature agarose, 0.25% bromphenol blue, and 40% sucrose], preheated to 70°C, were added. Mixed samples were electrophoresed on a 2% agarose gel containing 0.5 μg/ml ethidium bromide. DNA was visualized under UV illumination.

Caspase Activities. Caspase activity was determined using the Caspase-9/Mch6 Fluorometric Protease Assay Kit (MBL, Nagoya, Japan) and the ApoAlert CPP32/Caspase-3, FLICE/Caspase-8 Fluorescent Assay Kits (Clontech, Palo Alto, CA), according to the manufacturers' protocols. Briefly, 1×10^6 cells prepared from floating and attached cells 72 h after 10 Gy irradiation were lysed in reaction buffer containing 1 M DTT. Samples were then incubated with 50 μM AFC-conjugated substrates at 37°C for 60 min. We used Asp-Glu-Val-Asp (DEVD)-AFC, Ile-Glu-Thr-Asp (IETD)-AFC, and Leu-Glu-His-Asp (LEHD)-AFC substrates, respectively, to determine caspase-3-, -8-, and -9-like activities. The fluorescence intensity of AFC released from substrates was measured with a RF-540 spectrofluorometer (Shimadzu, Tokyo, Japan) equipped with 400 nm excitation and 505 nm emission filters. Enzyme activities were expressed as pmol AFC released/10^6 cells/h.

Colony-forming Assay. Clonogenic cell survival was evaluated by dose-survival curves as determined by a colony-forming assay. Immediately after γ-irradiation in plastic tubes at room temperature, cells were plated in 60-mm dishes and incubated at 37°C. After 7–10 days of incubation, cells were fixed and stained with crystal violet. Colonies containing >50 cells were counted, and the surviving fractions were then determined. To assess the effect of a PI3K inhibitor, we incubated cells plated in 60-mm dishes at 37°C for about 10 h. After 6 Gy of irradiation, cells were transferred to an incubator at 37°C and rendered to form colonies. The surviving fractions were determined as described above. Cell survival was corrected using the equation $S = 1 - (1 - f)^{1/N}$, where S is single cell survival, f is the measured surviving fraction, and N is the multiplicity determined by the average number of cells/microcolony at the time of irradiation. Multiplicity ranged from 1.1–1.2 for all cell lines under the described conditions.

Wortmannin Treatment. A PI3K inhibitor, wortmannin (Sigma Chemical Co., St. Louis, MO), was added to the medium at 0.1 and 1.0 μM 1 h before irradiation. To examine Akt/PKB activation, cells were lysed and processed for Western blotting after incubation at 37°C for the indicated times. In the colony-forming assay, wortmannin was present until fixation of cells.

γ-Irradiation. γ-Irradiation was performed using a ^{60}Co γ-ray therapeutic machine, RCR-120 (Toshiba, Tokyo, Japan), at a dose rate of 1.6 Gy/min.

Statistical Analysis. All data were expressed as the mean ± SE. The differences between groups were examined for statistical significance using the unpaired Student's t test. $P < 0.05$ denoted a statistically significant difference.

RESULTS

R+(Wt) and R+ Cells Express Similar Levels of the IGF-IR That Transduces Similar Phosphorylation Signals. Mouse embryo fibroblasts with a null mutation of the IGF-IR gene (R−) demonstrate IR-induced apoptosis, a process inhibited in IGF-IR-overexpressing cells (R+ cells) derived from R− cells (34). To precisely determine the relationship between apoptotic activity and clonogenic radiosensitivity, we established R+(Wt) cells, which express wild-type IGF-IR, and R−(puro) cells, which contain the control vector alone. The expression levels of the IGF-IR were determined by Western blots (Fig. 1*A*). The expression levels of IGF-IR in R+(Wt) and R+ cells were similar, as determined using antibodies against both the α- and β-subunits of the IGF-IR. Expression of protein kinase C-δ was examined as a control to demonstrate equal loading. The activity of the IGF-IR was examined by IGF-I-induced phosphorylation of the IGF-IR β-subunit and the major downstream substrates, IRS-1, a M_r 52,000 isoform of Shc, ERK-1, ERK-2, and Akt/PKB (Fig. 1*B*). No significant difference was observed in the intensity of each substrate activation between the two cell lines. Therefore, R+(Wt) and R+ cells express similar levels of the IGF-IR, transducing similar signals in response to IGF-I.

Characterization of *in Vitro* and *in Vivo* Growth. To examine the function of IGF-IR in cell proliferation, we constructed growth curves for monolayers of R−(puro), R+(Wt), and R+ cells (Fig. 2*A*). Both R+(Wt) and R+ cells grew faster than R−(puro) cells, confirming previous results (34). We then examined the tumorigenicity of these cell lines after s.c. inoculation into nude mice. Mouse embryo fibroblasts overexpressing IGF-IR exhibit a transformed phenotype under anchorage-independent conditions (29, 41). After the injection of R+ cells into mice, we detected a palpable mass within 1 week, which grew vigorously (Fig. 2*B*). These results were comparable to those obtained with NIH3T3 cells overexpressing IGF-IR (41). The tumor doubling time during exponential growth was approximately 2–3 days. In contrast, R−(puro) cells did not show significant tumorigenicity. Although a small mass ($V < 10$ mm^3) was palpable at approximately 8 weeks after inoculation, the tumor spontaneously regressed. Surprisingly, we found that R+(Wt) cells exhibited a delayed tumor appearance despite having similar IGF-IR expression levels as R+ cells (Fig. 1); a palpable mass was not detected until approximately 4 weeks after inoculation with an exponential growth phase doubling time of 6–7 days. R+ cells tended to grow faster than R+(Wt) cells in serum-free medium *in vitro*; conditioned medium derived from R+ cell cultures slightly stimulated the proliferation of R+(Wt) cells (data not shown). This soluble factor stimulat-

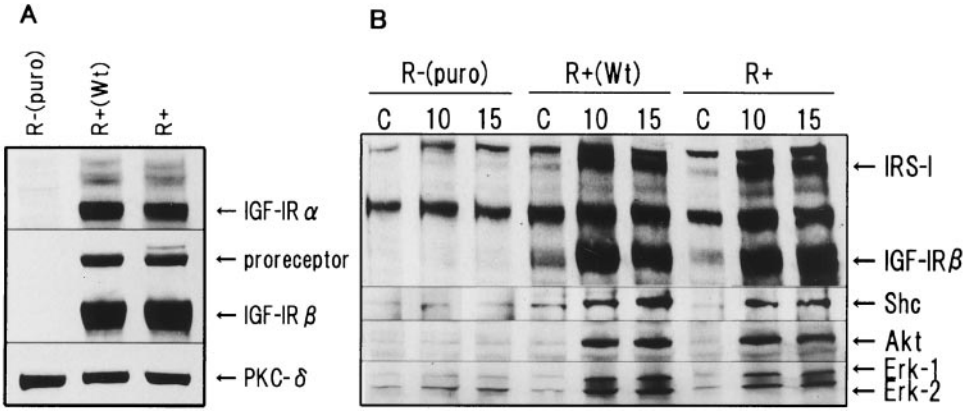

Fig. 1 Expression levels of the IGF-IR and IGF-I-induced phosphorylation of the major substrates in R−(puro), R+(Wt), and R+ cells. *A*, expression levels of IGF-IR in R+(Wt) and R+ cells. R−(puro), R+(Wt), and R+ cells were lysed; whole cell lysates were then subjected to SDS-PAGE as described in "Materials and Methods." Overexpressed IGF-IR was visualized using antibodies specific for α- and β-subunits of the IGF-IR. The IGF-IR proreceptor was also observed in blots using antibodies against the β-subunit. Protein kinase C-δ was used as a loading control. *B*, IGF-I-induced phosphorylation of the β-subunit of IGF-IR and the major substrates. Serum-starved cells in the presence or absence (*Lane C*) of 50 ng/ml IGF-I were lysed 10 or 15 min after stimulation. Equal amounts of cell lysates were separated using SDS-PAGE. The phosphorylated forms of IGF-IR β, IRS-1, Akt/PKB, ERK-1, and ERK-2 were detected using antibodies specific for phosphotyrosine, activated Akt, or activated MAPK as described in "Materials and Methods." To detect phosphorylated Shc, equal amounts of cell lysates were immunoprecipitated with an anti-Shc antibody and immunoblotted with an anti-phosphotyrosine antibody as described in "Materials and Methods."

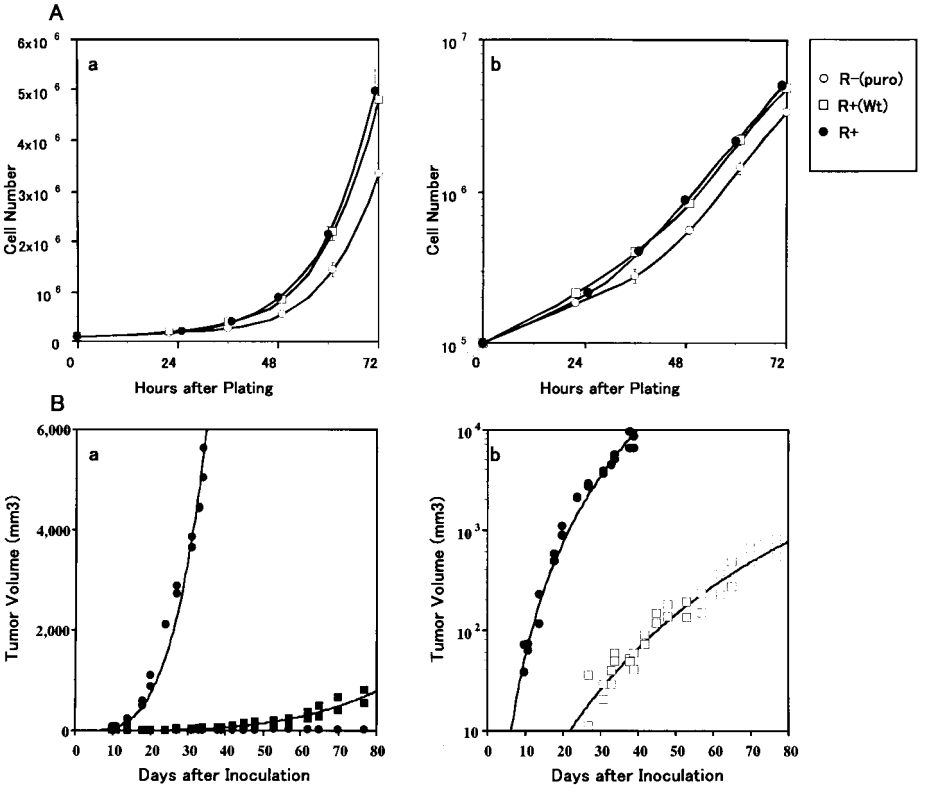

Fig. 2 Growth curves of R−(puro), R+(Wt), and R+ cells. *A*, growth curves in monolayer cultures. Cells (1×10^5) were plated in 60-mm dishes; the number of cells [displayed in either a linear (*a*), or logarithmic scale (*b*)] was determined by counting with a hemocytometer. The *bars* represent the mean ± SE of triplicate determinations from a representative experiment. *B*, growth curves of cells inoculated s.c. into nude mice. R−(puro), R+(Wt), and R+ cells (5×10^5 cells/100 μl) were injected into the right thigh of two nude mice each. The tumor size was measured using calipers; the volume was estimated as described in "Materials and Methods." Cell number or tumor volume was plotted in either a linear (*a*) or logarithmic scale (*b*) against time after inoculation.

ing cell growth may explain, at least in part, the vigorous tumor growth of R+ cells.

R+(Wt) Cells Do Not Exhibit Antiapoptotic Activity after γ-Irradiation. We examined the antiapoptotic effect of IGF-IR in R+(Wt) and R+ cells after γ-irradiation. After irradiation of R−(puro) cells at 10 Gy, significant numbers of cells detached from the dishes at about 48 h after irradiation. These cells exhibited DNA fragmentation characteristic of apoptosis, as demonstrated by agarose gel electrophoresis (Fig. 3*A*). None of the attached cells in the three cell lines demonstrated DNA

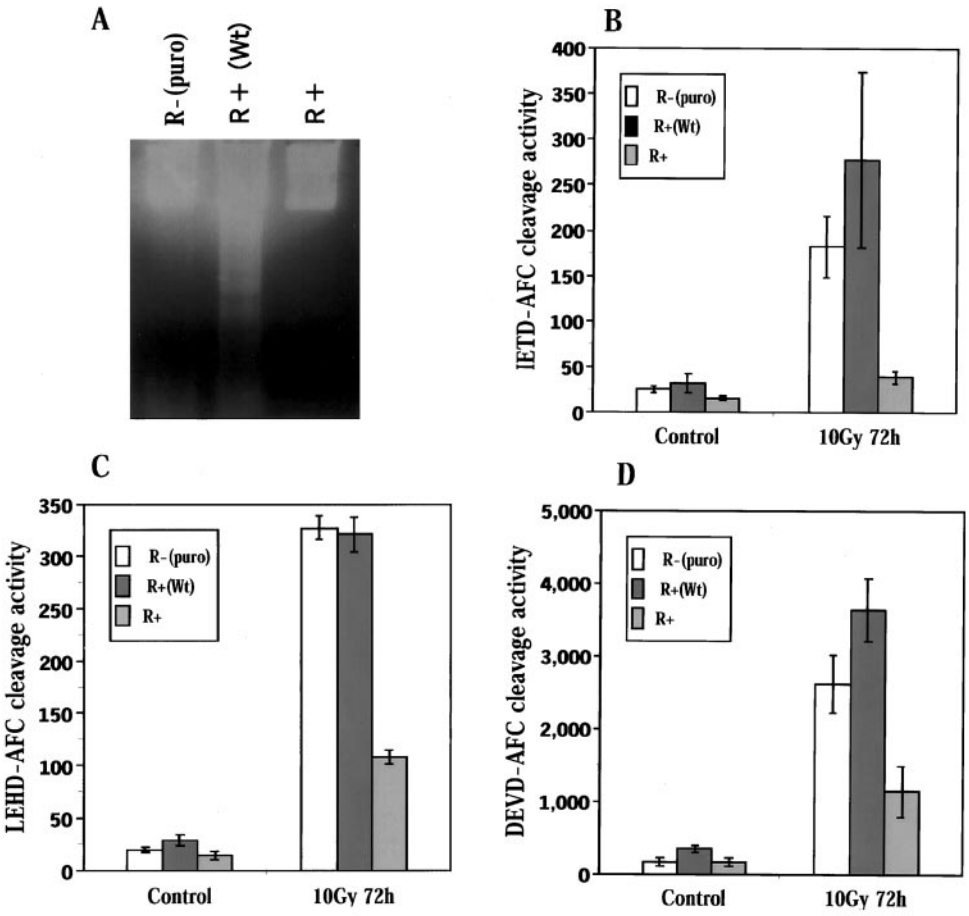

Fig. 3 Apoptotic features of R−(puro), R+(Wt), and R+ cells after γ-irradiation. *A*, γ-ray-induced DNA fragmentation. Cells were irradiated at a dose of 10 Gy; floating cells were collected 72 h after irradiation. DNA prepared as described in "Materials and Methods" was visualized by agarose gel electrophoresis. *B–D*, γ-ray-induced caspase activation. Seventy-two h after 10 Gy of irradiation, floating and attached cells were collected. We determined the activities of caspase-3-like (*D*), caspase-8-like (*B*), and caspase-9-like (*C*) proteases in cytosolic extracts using Asp-Glu-Val-Asp (DEVD)-AFC, Ile-Glu-Thr-Asp (IETD)-AFC, and Leu-Glu-His-Asp (LEHD)-AFC substrates, respectively. Cleavage activity is expressed as pmol AFC released/10^6 cells/h. Data are the mean ± SE of three independent experiments. Caspase activity after γ-irradiation was significantly increased in all samples as compared with nonirradiated cells in all cell lines (P was at least <0.02). γ-Ray-induced caspase activities in R−(puro) and R+(Wt) cells were significantly higher than those in R+ cells for all of the caspases examined (P was at least <0.02). No significant differences were observed between the caspase activities observed in R−(puro) and R+(Wt) cells.

fragmentation after irradiation (data not shown). Only a small number of floating R+ cells were detected; no evidence of apoptosis was evident in a DNA fragmentation assay, confirming previous findings (34). However, a larger number of floating R+(Wt) cells exhibited more DNA fragmentation than R−(puro) cells, demonstrating that the antiapoptotic effect present in R+ cells is lacking in both R+(Wt) and R−(puro) cells after γ-irradiation. Consistent with this finding, we observed significantly increased activation of the aspartate-specific cysteine protease family, the caspases (1–3, 6, 7), in R+(Wt) cells compared with R+ cells (Fig. 3, *B–D*); caspase activation is an essential step in the apoptotic pathway (1–3, 6, 7). Caspases are activated by cleavage at specific Asp residues; a model of hierarchical caspase activation proposes that activated caspase-8 and -9, which are termed the initiator caspases, activate the effector caspases, including caspase-3 and -7 (6). Therefore, R+ cells inhibit the caspase cascade upstream of the initiator caspases; this function is missing in R+(Wt) cells. The addition of 100 ng/ml IGF-I to 10% serum-containing medium did not inhibit γ-ray-induced apoptosis in R+(Wt) cells (data not shown). This result demonstrates that the autocrine mechanism operating in R+ cells is not likely to explain the differing antiapoptotic activities of the cell lines.

R+(Wt) Cells Exhibit a Similar Radioresistant Phenotype to R+ Cells in Terms of Clonogenic Survival. The three cell lines examined in this study differ with respect to IGF-IR expression and antiapoptotic activity. The radiation dose-survival curves obtained by colony-forming assay (Fig. 4) demonstrate that R+(Wt) cells are as radioresistant as R+ cells, although the former did not exhibit a significant antiapoptotic activity after γ-irradiation. These results indicate that in this cell system, overexpression of the IGF-IR mediates clonogenic radioresistance, regardless of antiapoptotic activity.

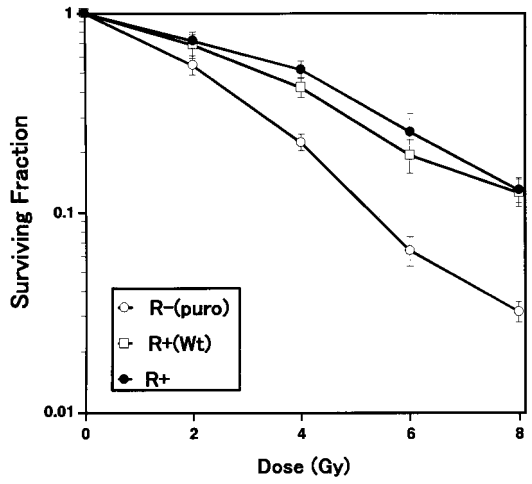

Fig. 4 Dose-survival curves in R−(puro) ○, R+(Wt) □, and R+ ● cells after γ-irradiation. The surviving fractions were determined by colony-forming assay as described in "Materials and Methods."

Time Course of MAPK and Akt/PKB Activation after γ-Irradiation. To identify the signal transduction mechanism associated with IGF-IR-mediated clonogenic radioresistance, we examined the activation of MAPK and Akt/PKB, two kinases functioning as downstream substrates of the IGF-IR to transduce survival signals (33). Although the activation of MAPK and Akt/PKB in serum-deprived R+(Wt) and R+ cells was similar after stimulation with IGF-I (Fig. 1*B*), the experimental conditions to determine clonogenic radiosensitivity by colony-forming assay were completely different; cells were always exposed to growth medium containing 10% serum, and IR induces MAPK activation primarily through EGFR without ligand stimulation (42). Endogenous EGFR expression levels were very low in R−(puro), R+(Wt), and R+ cells, but mRNA levels detected by reverse transcription-PCR and epidermal growth factor binding sites detected by the ^{125}I-epidermal growth factor binding assay were essentially the same among the three cell lines (data not shown). Although the effects of IGF-IR on IR-induced MAPK or Akt/PKB are unclear, we created experimental conditions in which MAPK and Akt/PKB activation can be monitored in 10% serum after γ-irradiation, as described in "Materials and Methods." The intensity of growth factor-induced phosphorylation peaks within 30 min and is subsequently attenuated by mechanisms such as internalization and ubiquitination (43–45). Cells chronically exposed to 10% serum exhibited low levels of MAPK (ERK-1 and ERK-2) and PKB/Akt activation, as compared with the levels 15 min after IGF-I stimulation (Fig. 5). MAPK stimulation was evident in R−(puro) cells 30 min after irradiation and persisted for up to 4 h (Fig. 5). No significant induction over control levels was detected in either R+(Wt) or R+ cells up to 4 h after irradiation, although steady-state activation levels were somewhat higher in these cell lines (Fig. 5). The activation of Akt/PKB was undetectable in R−(puro) cells; on the other hand, significant induction was observed in both R+(Wt) and R+ cells 30–60 min after irradiation and persisted for up to 4 h (Fig. 5). These findings suggest that Akt/PKB may mediate the clonogenic radioresistance observed in both R+(Wt) and R+ cells.

Inhibition of Akt/PKB by Wortmannin Exerts No Significant Effects on Clonogenic Radiosensitivity. To examine the effect of Akt/PKB inhibition on clonogenic radioresistance in R+(Wt) and R+ cells, we used a PI3K inhibitor, wortmannin, to inhibit Akt/PKB activity by inhibiting the upstream PI3K (46, 47). Akt/PKB activation in R+(Wt) and R+ cells after irradiation was undetectable after treatment with 0.1 or 1.0 μM wortmannin, although 0.1 μM wortmannin was unable to sufficiently inhibit IGF-I-induced Akt/PKB activation (Fig. 6*A*). We then examined the effect of this treatment on plating efficiency in all three cell lines. No cytotoxic effects were observed under these conditions (Fig. 6*B*). Because the half-maximal inhibitory concentration (IC_{50}) for DNA-PK or ATM in intact cells is ~5 μM (48, 49), the range used here is appropriate for studying the radiosensitizing effects of Akt/PKB inhibition, not DNA-PK or ATM inhibition. The results demonstrated that the inhibition of Akt/PKB does not affect clonogenic radioresistance in R+(Wt) and R+ cells (Fig. 6*C*). These results imply that the clonogenic radioresistance observed in R(Wt) and R+ cells is independent of PI3K-associated survival signals. Wortmannin at concentrations of 10 μM radiosensitized all three cell lines (data not shown), likely due to the inhibition of DNA-PK or ATM. These kinetics were consistent with reports by Sarkaria *et al.* (49) using A549 lung adenocarcinoma cells.

DISCUSSION

The enhancement of apoptosis in the radiotherapy of solid tumors will augment radioresponse and improve tumor outcomes, leading to higher survival rates. Assuming apoptosis is the major mode of cell death in tumors after IR, such an approach would prove highly effective; however, the role of apoptosis in radiotherapy must be verified when the incidence is low in the course of radiotherapy, as exemplified by solid tumors such as cervical carcinomas (25). Solid tumor cells die primarily by necrosis after IR; solid tumor cells may die by either necrosis or apoptosis (20). *In vitro* colony-forming assays, which are believed to reflect intrinsic radiosensitivity *in vivo*, have been used in radiobiology as a marker of the reproductive integrity of immortalized cells after IR (19, 39). Because this assay covers all types of cell death, we primarily evaluated the relationship between the induction of apoptosis and clonogenic radiosensitivity *in vitro* using mouse embryo fibroblast cell lines possessing the very two death components reported previously (34).

The major findings of the present study were as follows: (*a*) R+(Wt) and R+ cells, which express similar levels of IGF-IR, transduced similar IGF-I-induced phosphorylation signals to major downstream substrates; (*b*) both R+(Wt) and R+ cells, but not R−(puro) cells, demonstrated tumorigenic activity on s.c. inoculation into nude mice; however, R+(Wt) cells had a much longer tumor doubling time than R+ cells; (*c*) unlike R+ cells, R+(Wt) and R−(puro) cells lacked antiapoptotic activity after γ-irradiation; (*d*) R+(Wt) and R+ cells were both more radioresistant than R−(puro) cells as determined by colony-forming assay; (*e*) γ-irradiation induced Akt/PKB activa-

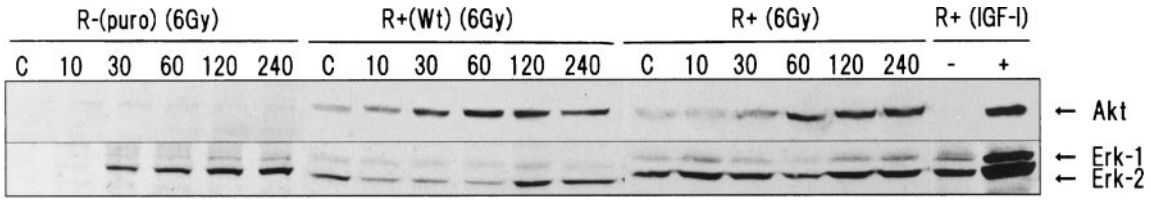

Fig. 5 Time-course study of γ-ray-induced activation of MAPK and Akt/PKB in R−(puro), R+(Wt), and R+ cells. Cells grown in 10% serum were irradiated at 6 Gy and then lysed after an incubation at 37°C for the indicated times (in minutes). Equal amounts of whole cell lysates were subjected to SDS-PAGE; activated MAPK and Akt/PKB were visualized as described in "Materials and Methods." Activation of MAPK and Akt/PKB in R+ cells 15 min after stimulation with (+) or without 50 ng/ml IGF-I (−) is also displayed.

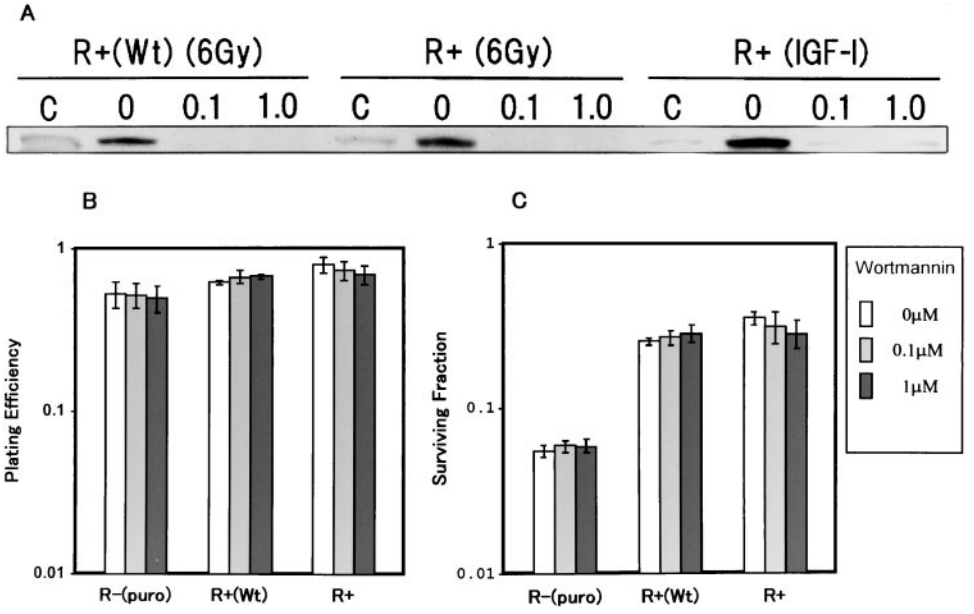

Fig. 6 Effect of a PI3K inhibitor on both γ-ray-induced activation of Akt/PKB and clonogenic radiosensitivity of R+(Wt) and R+ cells. *A*, inhibition of γ-ray-induced activation of Akt/PKB by a PI3K inhibitor, wortmannin. Cells were incubated in the presence or absence of 0.1 or 1.0 μM wortmannin in 10% serum for 1 h and then irradiated at 6 Gy. After incubation at 37°C for either 60 [R+(Wt)] or 120 min (R+), cells were lysed; activated Akt/PKB was visualized as described in "Materials and Methods." The results of the effects of wortmannin on IGF-I (50 ng/ml)-induced Akt/PKB activation 15 min after stimulation are also shown. *Lane C*, untreated control; *Lane 0*, cells not treated with wortmannin before irradiation; *Lanes 0.1* and *1.0*, cells treated with 0.1 or 1.0 μM wortmannin before irradiation. *B* and *C*, effect of wortmannin on both plating efficiency and clonogenic survival in R−(puro), R+(Wt), and R+(Wt) cells after γ-irradiation. An appropriate number of cells grown in dishes were either left untreated or treated with 0.1 or 1.0 μM wortmannin in 10% serum for 1 h and irradiated at 6 Gy. Cells were allowed to form colonies at 37°C in the presence of wortmannin. The multiplicity-corrected surviving fraction was determined as described in "Materials and Methods."

tion in both R+(Wt) and R+ cells with similar time courses, but no activation was observed in R−(puro) cells; and (*f*) wortmannin inhibited γ-ray-induced Akt/PKB activation without altering clonogenic radioresistance in R+(Wt) and R+ cells at concentrations specifically inhibiting PI3K.

R+(Wt) and R+ cells exhibited similar clonogenic radioresistance compared with R−(puro) cells, irrespective of the apoptotic activity observed after γ-irradiation. This kind of discrepancy was not restricted to our *in vitro* model but was also observed after radiation or chemotherapeutic treatment in colon cancer cell lines with targeted disruption of the *p53* or *p21* genes (50, 51). After the combined therapy of surgery and radiation, patients with breast cancer expressing higher levels of IGF-IR had significantly higher recurrence rates than those expressing lower levels of IGF-IR, although this study lacked information on apoptosis induction (30). There is still a gap between our *in vitro* data and clinical results, however, the accumulated *in vitro* evidence provides clinical implications in the evaluation of apoptotic activity observed during radiotherapy of solid tumors to predict accurate tumor response or local control.

The mechanism whereby R+(Wt) and R+ cells, in contrast to R−(puro) cells, develop clonogenic radioresistance regardless of their antiapoptotic activity remains unclear. McCarthy *et al.* (52) suggest that Bcl-2 and IGF-I suppress the initiation of apoptosis but exert no effect on the apoptotic program once it is initiated. Activation of the IGF-IR may therefore suppress the initiation of cell death upstream of the irreversible point at which a cell becomes committed to death (52). Overexpression of the IGF-IR thus increases the number of surviving cells to a similar extent in R+(Wt) and R+ cells, as determined by

clonogenic assay. The mode of cell death may be determined downstream of the crucial point; therefore, the mechanism inducing apoptosis in R+(Wt) cells and necrosis in R+ cells after this crucial initiation step may function as a part of the death pathway in conjunction with the IGF-IR. Tumor necrosis factor α-induced caspase activation has both proapoptotic and antinecrotic effects; inhibition of caspase activity induces massive necrotic cell death (53). The existence of regulatory mechanisms involved in determining the mode of cell death is likely; the difference between R+(Wt) and R+ cells may be attributed to such mechanisms. Variations in EGFR levels or autocrine effects between the cell lines are unlikely to mediate this effect.

Because overexpression of the IGF-IR commonly induced clonogenic radioresistance in both R+(Wt) and R+ cells, we secondarily pursued the type of IGF-IR signals related to clonogenic radioresistance. We focused on MAPK and PI3K-associated pathways because they are the major survival signals originating from the IGF-IR (32, 33, 54, 55). Signal activation was monitored in growth medium because the determination of radiosensitivity requires 10% serum. The contribution of MAPK could be excluded because significant MAPK activation was observed even in R−(puro) cells after irradiation (Fig. 5). The IGF-IR activates IRS-1, which in turn activates PI3K, to activate Akt/PKB (54). The concluding step is the phosphorylation of BAD, a member of Bcl-2 family, by Akt/PKB (32). Phosphorylated BAD fails to form a complex with Bcl-x_L, allowing the homodimer of Bcl-x_L to suppress caspase-9 activation (56). In our study, γ-irradiation similarly activated Akt/PKB in both R+(Wt) and R+ cells, but not in R−(puro) cells (Fig. 5). We therefore examined the possible role of the signals involved in clonogenic radioresistance; inhibition of PI3K through wortmannin treatment had no effect on the clonogenic radiosensitivity of either R+(Wt) or R+ cells (Fig. 6). These results suggest that the clonogenic radioresistance observed in R+(Wt) and R+ cells is mediated by PI3K-independent survival signals. To evaluate the existence of additional signals closely related to IGF-IR-mediated clonogenic radioresistance, studies using mutant IGF-IRs are now under way.

We have demonstrated that apoptotic activity may not necessarily reflect clonogenic radiosensitivity *in vitro*, indicating that the information obtained regarding apoptosis during radiotherapy should be carefully interpreted to predict accurate tumor response or local control. Furthermore, our findings suggest the possibility that unique IGF-IR signaling pathways dissociated from antiapoptotic signals may lead to clonogenic survival.

ACKNOWLEDGMENTS

We thank Dr. I. Morita for help in measuring caspase activities and Dr. R. Baserga for critical reading of the manuscript.

REFERENCES

1. Alnemri, E. S. Mammalian cell death proteases: a family of highly conserved aspartate specific cysteine proteases. J. Cell. Biochem., *64:* 33–42, 1997.

2. Cohen, G. M. Caspases: the executioners of apoptosis. Biochem. J., *326:* 1–16, 1997.

3. Salvesen, G. S., and Dixit, V. M. Caspases: intracellular signaling by proteolysis. Cell, *91:* 443–446, 1997.

4. Wyllie, A. H., Morris, R. G., Smith, A. L., and Dunlop, D. Chromatin cleavage in apoptosis: association with condensed chromatin morphology and dependence on macromolecular synthesis. J. Pathol., *142:* 67–77, 1984.

5. Yamada, T., and Ohyama, H. Radiation-induced interphase death of rat thymocytes is internally programmed (apoptosis). Int. J. Radiat. Biol. Relat. Stud. Phys. Chem. Med., *53:* 65–75, 1988.

6. Slee, E. A., Harte, M. T., Kluck, R. M., Wolf, B. B., Casiano, C. A., Newmeyer, D. D., Wang, H. G., Reed, J. C., Nicholson, D. W., Alnemri, E. S., Green, D. R., and Martin, S. J. Ordering the cytochrome *c*-initiated caspase cascade: hierarchical activation of caspases-2, -3, -6, -7, -8, and -10 in a caspase-9-dependent manner. J. Cell Biol., *144:* 281–292, 1999.

7. Nicholson, D. W., and Thornbery, N. A. Caspases: killer proteases. Trends Biochem. Sci., *22:* 299–307, 1997.

8. Wyllie, A. H., Kerr, J. F. R., and Currie, A. R. Cell death: the significance of apoptosis. Int. Rev. Cytol., *68:* 251–306, 1980.

9. Baringa, M. Death gives birth to the nervous system. But how? Science (Wash. DC), *259:* 762–763, 1993.

10. Monti, D., Troiano, L., Tropea, F., Grassilli, E., Cossarizza, A., Bellomo, G., and Franceshi, C. Apoptosis–programmed cell death: a role in the aging process. Am. J. Clin. Nutr., *55:* 1208S–1214S, 1992.

11. Wyllie, A. H. Glucocorticoid-induced thymocyte apoptosis is associated with endogenous endonuclease activation. Nature (Lond.), *284:* 555–556, 1980.

12. Kawasaki, H., Morooka, T., Shimohama, S., Kimura, J., Hirano, T., Gotoh, Y., and Nishida, E. Activation and involvement of p38 mitogen-activated protein kinase in glutamate-induced apoptosis in rat cerebellar granule cells. J. Biol. Chem., *272:* 18518–18521, 1997.

13. Butterfield, L., Storey, B., Maas, L., and Heasley, L. E. c-Jun NH_2-terminal kinase regulation of the apoptotic response of small cell lung cancer cells to ultraviolet radiation. J. Biol. Chem., *272:* 10110–10116, 1997.

14. Chen, Y. R., Meyer, C. F., and Tan, T. H. Persistent activation of c-jun N-terminal kinase 1 (JNK1) in γ radiation-induced apoptosis. J. Biol. Chem., *271:* 631–634, 1996.

15. Chen, Y. R., Wang, X., Templeton, D., Davis, R. J., and Tan, T. H. The role of c-Jun NH_2-terminal kinase (JNK) in apoptosis induced by ultraviolet C and γ radiation. Duration of JNK activation may determine cell death and proliferation. J. Biol. Chem., *271:* 31929–31936, 1996.

16. Chen, Z., Seimiya, H., Naito, M., Mashima, T., Kizaki, A., Dan, S., Imaizumi, M., Ichijo, H., Miyazono, K., and Tsuruo, T. ASK1 mediates apoptotic cell death induced by genotoxic stress. Oncogene, *18:* 173–180, 1999.

17. Williams, G. T. Programmed cell death: apoptosis and oncogenesis. Cell, *65:* 1097–1098, 1991.

18. Woo, M., Hakem, R., Soengas, M. S., Duncan, G. S., Shahinian, A., Kagi, D., Hakem, A., McCurrach, M., Khoo, W., Kaufman, S. A., Senaldi, G., Howard, T., Lowe, S. W., and Mak, J. R. Essential contribution of caspase 3/CPP32 to apoptosis and its associated nuclear change. Genes Dev., *12:* 806–819, 1998.

19. Dewey, W. C., Ling, C. C., and Meyn, R. E. Radiation-induced apoptosis: relevance to radiotherapy. Int. J. Radiat. Oncol. Biol. Phys., *33:* 781–796, 1995.

20. Finkel, E. Does cancer therapy trigger cell suicide? Science (Wash. DC), *286:* 2256–2258, 1999.

21. Stephens, L. C., Hunter, N. R., Ang, K. K., Milas, L., and Meyn, R. E. Development of apoptosis in irradiated murine tumors as a function of time and dose. Radiat. Res., *135:* 75–80, 1993.

22. Wheeler, J. A., Stephens, L. C., Tornos, C., Eifel, P. J., Ang, K. K., Milas, L., Allen, P. K., and Meyn, R. E. Apoptosis as a predictor of tumor response to radiation in stage IB cervical carcinoma. Int. J. Radiat. Oncol. Biol. Phys., *32:* 1487–1493, 1995.

23. Paxton, J. R., Bolger, B. S., Armour, A., Symonds, R. P., Mao, J. H., and Burnett, R. A. Apoptosis in cervical squamous carcinoma: predictive value for survival following radiotherapy. J. Clin. Pathol., *53:* 197–200, 2000.

24. Levine, E. L., Davidson, S. E., Roberts, S. A., Chadwick, C. A., Potten, C. S., and West, C. M. L. Apoptosis as predictor of response to radiotherapy in cervical carcinoma. Lancet, *344:* 472–473, 1994.

25. Yuki, H., Fujiwara, M., Yamakawa, Y., Hidaka, T., and Saito, S. Detection of apoptosis and expression of apoptosis-associated proteins as early predictors of prognosis after irradiation therapy in stage IIIb uterine cervical cancer. Jpn. J. Cancer Res., *91:* 127–134, 2000.

26. Sell, C., Rubini, M., Rubin, R., Liu, J. P., Efstratiadis, A., and Baserga, R. Simian virus 40 large tumor antigen is unable to transform mouse embryo fibroblasts lacking type-1 IGF receptor. Proc. Natl. Acad. Sci. USA, *90:* 11217–11221, 1993.

27. Sell, C., Dumenil, G., Deveaud, C., Miura, M., Coppola, D., DeAngelis, T., Rubin, R., Efstrariadis, A., and Baserga, R. Effect of a null mutation of the insulin-like growth factor I receptor gene on growth and transformation of mouse embryo fibroblasts. Mol. Cell. Biol., *14:* 3604–3612, 1994.

28. O'Connor, R., Kauffmann-Zeh, A., Liu, Y., Lehar, S., Evan, G. I., Baserga, R., and Blattler, W. A. Identification of domains of the insulin-like growth factor I receptor that are required for protection from apoptosis. Mol. Cell. Biol., *17:* 427–435, 1997.

29. Baserga, R. The price of independence. Exp. Cell Res., *236:* 1–3, 1997.

30. Turner, B. C., Haffty, B. G., Narayanan, L., Yuan, J., Havre, P. A., Gumbs, A. A., Kaplan, L., Burgaud, J. L., Carter, D., Baserga, R., and Glazer, P. M. Insulin-like growth factor I receptor overexpression mediates cellular radioresistance and local breast cancer recurrence after lumpectomy and radiation. Cancer Res., *57:* 3079–3083, 1997.

31. Merrill, M. J., and Edwards, N. A. Insulin-like growth factor-I receptors in human glial tumors. J. Clin. Endocrinol. Metab., *70:* 199–209, 1990.

32. Datta, S. R., Dudek, H., Tao, X., Masters, S., Fu, H., Gotoh, Y., and Greenberg, M. E. Akt phosphorylation of BAD couples survival signals to the cell-intrinsic death machinery. Cell, *91:* 231–241, 1997.

33. Peruzzi, F., Prisco, M., Dews, M., Salomoni, P., Grassilli, E., Romano, G., Calabretta, B., and Baserga, R. Multiple signaling pathways of the insulin-like growth factor 1 receptor in protection from apoptosis. Mol. Cell. Biol., *19:* 7203–7215, 1999.

34. Nakamura, S., Watanabe, H., Miura, M., and Sasaki, T. Effect of the insulin-like growth factor I receptor on ionizing radiation-induced cell death in mouse embryo fibroblasts. Exp. Cell Res., *235:* 287–294, 1997.

35. Miura, M., Surmacz, E., Burgaud, J. L., and Baserga, R. Different effects on mitogenesis and transformation of a mutation at tyrosine 1251 of the insulin-like growth factor I receptor. J. Biol. Chem., *270:* 22639–22644, 1995.

36. Hongo, A., D'Ambrosio, C., Miura, M., Morrione, A., and Baserga, R. Mutational analysis of the mitogenic and transforming activities of the insulin-like growth factor I receptor. Oncogene, *12:* 1231–1238, 1996.

37. Stewart, C. E. H., Newcomb, P. V., Savage, P. B., Dickens, M., Tavare, J., and Holly, J. M. P. Increased, not decreased, activation of the insulin-like growth factor (IGF) receptor signalling pathway during ceramide-induced apoptosis. Growth Horm. IGF Res., *9:* 131–142, 1999.

38. Nakamura, K., Hongo, A., Kodama, J., Miyagi, Y., Yoshinouchi, M., and Kudo, T. Down-regulation of the insulin-like growth factor I receptor by antisense RNA can reverse the transformed phenotype of human cervical cancer cell lines. Cancer Res., *60:* 760–765, 2000.

39. Hall, E. J. Radiobiology for the Radiologist, 5th ed., pp. 32–50. Philadelphia: J. B. Lippincott Co., 1994.

40. de la Luna, S., Soria, I., Pulido, D., Ortin, J., and Jimenez, A. Efficient transformation of mammalian cells with constructs containing a puromycin-resistance marker. Gene (Amst.), *62:* 121–126, 1988.

41. Butler, A. A., Blakesley, V. A., Tsokos, M., Pouliki, V., Wood, T. L., and LeRoith, D. Stimulation of tumor growth by recombinant human insulin-like growth factor-I (IGF-I) is dependent on the dose and the level of IGF-I receptor expression. Cancer Res., *58:* 3021–3027, 1998.

42. Schmidt-Ullrich, R. K., Mikkelsen, R. B., Dent, P., Todd, D. G., Valerie, K., Kavanagh, B. D., Contessa, J. N., Rorrer, W. K., and Chen, P. B. Radiation-induced proliferation of the human A431 squamous cell carcinoma cells is dependent on EGFR tyrosine phosphorylation. Oncogene, *15:* 1191–1197, 1997.

43. Chen, W. S., Lazar, C. S., Lund, K. A., Welsh, J. B., Chang, C-P., Walton, G. M., Der, C. J., Wiley, H. S., Gill, G. N., and Rosenfeld, M. G. Functional independence of the epidermal growth factor from a domain required for ligand-induced internalization and calcium regulation. Cell, *59:* 33–43, 1989.

44. Miura, M., and Baserga, R. The tyrosine residue at 1250 of the insulin-like growth factor I receptor is required for ligand-mediated internalization. Biochem. Biophys. Res. Commun., *239:* 182–185, 1997.

45. Zhang, H., Hoff, H., and Sell, C. Insulin-like growth factor I-mediated degradation of insulin receptor substrate-1 is inhibited by epidermal growth factor in prostate epithelial cells. J. Biol. Chem., *275:* 22558–22562, 2000.

46. Kapellar, R., and Cantley, C. Phosphatidylinositol 3-kinase. Bioessays, *16:* 565–576, 1994.

47. Nunoi, K., Yasuda, K., Tanaka, H., Kubota, A., Okamoto, Y., Adachi, T., Shihara, N., Uno, M., Xu, L. M., Kagimoto, S., Seino, Y., Yamada, Y., and Tsuda, K. Wortmannin, a PI3-kinase inhibitor: promoting effect on insulin secretion from pancreatic β cells through a cAMP-dependent pathway. Biochem. Biophys. Res. Commun., *270:* 798–805, 2000.

48. Izzard, R. A., Jackson, S. P., and Smith, G. C. Competitive and non-competitive inhibition of the DNA-dependent protein kinase. Cancer Res., *59:* 2581–2586, 1999.

49. Sarkaria, J. N., Tibbetts, R. S., Busby, E. C., Kennedy, A. P., Hill, D. E., and Abraham, R. T. Inhibition of phosphoinositide 3-kinase-related kinases by the radiosensitizing agent wortmannin. Cancer Res., *58:* 4375–4382, 1998.

50. Waldman, T., Zhang, Y., Dillehay, L., Yu, J., Kinzler, K., Vogelstein, B., and Williams, J. Cell cycle arrest *versus* cell death in cancer therapy. Nat. Med., *3:* 1034–1036, 1997.

51. Bunz, F., Hwang, P. M., Torrance, C., Waldman, T., Zhang, Y., Dillehay, L., Williams, J., Lengauer, C., Kinzler, K. W., and Vogelstein, B. Disruption of p53 in human cancer cells alters the responses to therapeutic agents. J. Clin. Investig., *104:* 263–269, 1999.

52. McCarthy, N. J., Whyte, M. K. B., Gilbert, C. S., and Evan, G. I. Inhibition of Ced3/ICE-related proteases does not prevent cell death induced by oncogenes, DNA damage, or Bcl-2 homologue Bak. J. Cell Biol., *136:* 215–227, 1997.

53. Khwaja, A., and Tatton, L. Resistance to the cytotoxic effects of tumor necrosis factor α can be overcome by inhibition of a FADD/caspase-dependent signaling pathway. J. Biol. Chem., *274:* 36817–36823, 1999.

54. Kulik, G., and Weber, J. Antiapoptotic signaling by the insulin-like growth factor I receptor, phosphatidylinositol 3-kinase, and Akt. Mol. Cell. Biol., *17:* 1595–1606, 1997.

55. Kulik, G., and Weber, J. Akt-dependent and -independent survival signaling pathways utilized by insulin-like growth factor I. Mol. Cell. Biol., *18:* 6711–6718, 1998.

56. Zha, J., Harada, H., Yang, E., Jockel, J., and Korsmeyer, S. J. Serine phosphorylation of death agonist Bad in response to survival factor results in binding to 14.3.3 not Bcl-x_L. Cell, *87:* 619–628, 1996.

Clinical Cancer Research

Antiapoptotic Activity Is Dispensable for Insulin-like Growth Factor I Receptor-mediated Clonogenic Radioresistance after γ -Irradiation

Mikio Tezuka, Hiroshi Watanabe, Shin Nakamura, et al.

Clin Cancer Res 2001;7:3206-3214.